





RESEARCH ARTICLE

CSGALNACT1-congenital disorder of glycosylation: A mild skeletal dysplasia with advanced bone age

Shuji Mizumoto^{1,2*} | Andreas R. Janecke^{3,4*}  | Azita Sadeghpour⁵ | Gundula Povysil⁶ | Marie T. McDonald⁷ | Sheila Unger⁸ | Susanne Greber-Platzer⁹ | Kristen L. Deak¹⁰ | Nicholas Katsanis^{5,11,12}  | Andrea Superti-Furga¹³ | Kazuyuki Sugahara¹ | Erica E. Davis^{5,11,12}  | Shuhei Yamada¹ | Julia Vodopiutz⁹ 

¹Department of Pathobiochemistry, Faculty of Pharmacy, Meijo University, Nagoya, Japan

²Department of Women's and Children's Health, Clinical Genetics Group, Dunedin School of Medicine, University of Otago, Dunedin, New Zealand

³Department of Pediatrics I, Medical University of Innsbruck, Innsbruck, Austria

⁴Division of Human Genetics, Medical University of Innsbruck, Innsbruck, Austria

⁵Center for Human Disease Modeling, Duke University Medical Center, Durham, North Carolina

⁶Institute of Bioinformatics, Johannes Kepler University, Linz, Austria

⁷Department of Pediatrics, Division of Medical Genetics, Duke University Medical Center, Durham, North Carolina

⁸Department of Medical Genetics, Centre Hospitalier Universitaire Vaudois, University of Lausanne, Lausanne, Switzerland

⁹Department of Pediatrics and Adolescent Medicine, Comprehensive Center for Pediatrics, Medical University of Vienna, Vienna, Austria

¹⁰Department of Pathology, Duke University Medical Center, Durham, North Carolina

¹¹Advanced Center for Translational and Genetic Medicine (ACT-GeM), Stanley Manne Children's Research Institute, Ann & Robert H. Lurie Children's Hospital of Chicago, Chicago, Illinois

¹²Department of Pediatrics, Feinberg School of Medicine, Northwestern University, Chicago, Illinois

¹³Department of Pediatrics, Centre Hospitalier Universitaire Vaudois, University of Lausanne, Lausanne, Switzerland

Correspondence

Julia Vodopiutz, Department of Pediatrics and Adolescent Medicine, Comprehensive Center for Pediatrics Medical University of Vienna, Währinger Gürtel 18-20, A-1090 Wien, Austria.

Email: julia.vodopiutz@meduniwien.ac.at

Funding information

NIH Clinical Center, Grant/Award Numbers: DK096415 (to N. K.), MH106826 (to E. E. D.); Jubiläumsfond Oesterreichische Nationalbank, Grant/Award Number: Nr17627 (to J. V.); Japan Society for the Promotion of Science, Grant/Award Numbers: 16K08251 (to S. M.), 19K07054 (to S. M.); Takeda Science Foundation (to S. M.)

Abstract

Congenital disorders of glycosylation (CDGs) comprise a large number of inherited metabolic defects that affect the biosynthesis and attachment of glycans. CDGs manifest as a broad spectrum of disease, most often including neurodevelopmental and skeletal abnormalities and skin laxity. Two patients with biallelic *CSGALNACT1* variants and a mild skeletal dysplasia have been described previously. We investigated two unrelated patients presenting with short stature with advanced bone age, facial dysmorphism, and mild language delay, in whom trio-exome sequencing identified novel biallelic *CSGALNACT1* variants: compound heterozygosity for c.1294G>T (p.Asp432Tyr) and the deletion of exon 4 that includes the start codon in one patient, and homozygosity for c.791A>G (p.Asn264Ser) in the other patient. *CSGALNACT1* encodes CSGalNAcT-1, a key enzyme in the biosynthesis of sulfated glycosaminoglycans chondroitin and dermatan sulfate. Biochemical studies demonstrated significantly reduced CSGalNAcT-1 activity of the novel missense variants, as

*Shuji Mizumoto and Andreas R. Janecke are joint first authors.

reported previously for the p.Pro384Arg variant. Altered levels of chondroitin, dermatan, and heparan sulfate moieties were observed in patients' fibroblasts compared to controls. Our data indicate that biallelic loss-of-function mutations in *CSGALNACT1* disturb glycosaminoglycan synthesis and cause a mild skeletal dysplasia with advanced bone age, *CSGALNACT1*-CDG.

KEYWORDS

advanced bone age, cartilage and brain development, *CSGalNAcT-1*, *CSGALNACT1*-CDG, glycosaminoglycan, joint laxity, macrocephaly, proteoglycan, short stature

1 | INTRODUCTION

Congenital disorders of glycosylation (CDGs) are monogenic inherited conditions that result from abnormal glycan biosynthesis resulting in a broad spectrum of pathologies. These clinical entities often include skin laxity, skeletal dysplasias, neurodevelopmental disorders, and endocrine abnormalities. So far, more than 125 different CDG have been identified among several glycosylation pathways (Bui et al., 2014; Ng & Freeze, 2018). One of these pathways is the O-linked xylose (O-Xyl) glycosylation pathway, which is governed by several genes that encode enzymes responsible for the biosynthesis and structural diversity of sulfated glycosaminoglycans (GAGs; Mizumoto, 2018; Mizumoto, Yamada, & Sugahara, 2015b).

GAGs are unbranched polysaccharides that form the side chains of proteoglycans (PGs) and have been classified into chondroitin sulfate (CS), dermatan sulfate (DS), and heparan sulfate (HS), based on their repeating disaccharide units. GAGs are a major component of the extracellular matrix, play an important role in cartilage and brain development, and are critical for the mechanical properties of connective tissue (Bishop, Schuksz, & Esko, 2007; Haltiwanger & Lowe, 2004; Ida-Yonemochi et al., 2018; Mizumoto, Yamada, & Sugahara, 2015a; Sato et al., 2011; Watanabe et al., 2010). The biosynthesis of GAGs starts with the formation of a common tetrasaccharide linker region, which is attached covalently to the serine residues of the PG core proteins (Lindahl & Rodén, 1965). Four glycosyltransferases subsequently polymerize the common tetrasaccharide linker region in CS, DS, and HS biosynthesis. This is followed by the stepwise polymerization of either HS or CS/DS chains. The first hexosamine transfer to the tetrasaccharide linker region determines selectively whether HS or CS/DS is produced. CS *N*-acetylgalactosaminyltransferase-1 (*CSGalNAcT-1*, ChGn-1) encoded by *CSGALNACT1* (MIM# 616615) initiates CS/DS synthesis by catalyzing the transfer of a GalNAc residue from uridine diphosphate (UDP)-GalNAc onto the tetrasaccharide linker (Izumikawa et al., 2015; Uyama, Kitagawa, Tamura Ji, & Sugahara, 2002).

Recently, we and others reported two patients with biallelic *CSGALNACT1* variants and a mild skeletal dysplasia with advanced bone age (Meyer et al., 2019; Vodopiutz et al., 2017). Here, we report two additional affected individuals with biallelic *CSGALNACT1* variants and we show altered GAG synthesis in fibroblasts from one patient. We hereby suggest that *CSGALNACT1* loss-of-function causes a distinct disease entity, the congenital disorder of glycosylation, *CSGALNACT1*-CDG.

2 | PATIENTS AND METHODS

2.1 | Patients

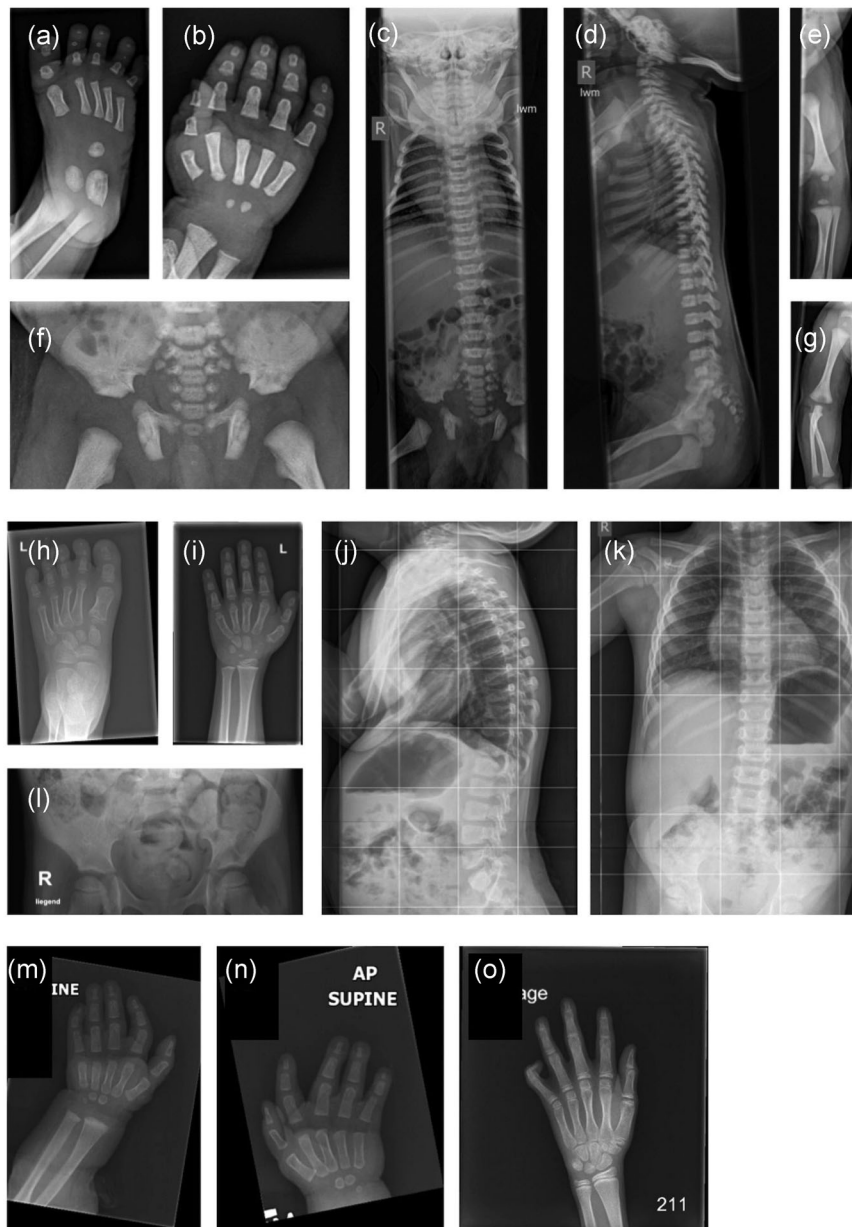
Two patients (P2, P3) with skeletal dysplasia with advanced carpal bone age in infancy (Figures 1a–o and 2a–c), were examined by consultants specialized in pediatrics, radiology, and clinical genetics. Sharing of patient-related data was facilitated by the GeneMatcher tool (Sobreira, Schiettecatte, Valle, & Hamosh, 2015). Fibroblasts from patient P2 and from the previously reported patient (P1) with *CSGalNAcT-1* deficiency (Vodopiutz et al., 2017) were studied. Written informed consent for genetic and metabolic research investigations was obtained from all participants, and the ethics committees of the Medical University of Innsbruck, Austria (P1), Medical University of Vienna (P2), Duke University Health System (P3), and of the Meijo University, Nagoya, Japan, approved the study. Genomic DNA was extracted from peripheral blood from all participants by standard procedures.

2.2 | Whole-exome sequencing (WES)

WES was performed on patient P2 and his parents using the Sureselect V6 exome enrichment kit (Agilent Technologies, Waldbronn, Germany) and the 150 bp (base pairs) paired-end mode on an Illumina HiSeq4000 instrument (GATC-Biotech, Konstanz, Germany). Sequencing reads were aligned to the human genome (hg19) with Burrows-Wheeler transformation (Li & Durbin, 2009), polymerase chain reaction (PCR) duplicates removed with PICARD (<http://picard.sourceforge.net>), and single-nucleotide variants (SNVs) and small indels were identified with the samtools mpileup software. All variants were submitted to SeattleSeq (<http://snp.gs.washington.edu/SeattleSeqAnnotation/>) for annotation, categorization into synonymous and nonsynonymous SNPs or indels, and for filtering using the data from dbSNP, the Exome Sequencing Project (ESP), and the Exome Aggregation consortium (ExAC), genome aggregation database (gnomAD). A spreadsheet-based filtering for rare and private variants was performed. Copy-number variants (CNVs) were detected using the panelcn.MOPS software package (Povysil et al., 2017).

WES was performed on patient P3 and her parents as described (Jordan et al., 2015) with VCRome 2.1 in-solution exome probes (Bainbridge et al., 2011) and 100 bp paired-end reads on an Illumina HiSeq 4000 instrument; data were processed with CASAVA 1.8

FIGURE 1 Radiological features in two unrelated patients with CSGALNACT1-CDG. (a–g) Neonatal skeletal radiographs in P2 showing: (a, b) advanced carpotarsal bone age; (a–e, g) short and plump long bones, narrow chest, and coronal clefting of vertebrae; and (f) trident-shaped acetabula, and monkey wrench appearance of the proximal femur. (h–l) Follow-up skeletal radiographs in P2 showing scoliosis and pectus excavatum: (h, i, l) age 4 years and 10 months; (j, k) age 3 years and 10 months. (m–o) Mildly advanced bone age in P3 at the age of 7 months (m, n); vanishing by the age of 9 years and 9 months (o)



software (Illumina), and mapped to the reference human genome (hg19) with BWA (Li & Durbin, 2009). Variant calls were performed using Atlas-SNP and Atlas-indel (Shen et al., 2010), and data were filtered to retain functional variants predicted to alter messenger RNA (mRNA) splicing or protein amino acid sequence with minor allele frequency $\leq 1\%$ in public SNP databases (dbSNP, ESP, ExAC, and gnomAD) that segregated with disease.

2.3 | Sanger sequencing and quantitative PCR

SNVs and CNVs detected by WES were confirmed by Sanger sequencing and quantitative PCR, respectively, using an ABI 3730s automated sequencer, with BigDye terminator mix and an ABI real-time PCR cyclor. CSGALNACT1 PCR and sequencing primer sequences were based on the ENSEMBL reference entries for mRNA (ENST00000454498.2, corresponding to NCBI reference sequence for mRNA NM_001130518.1), and

genomic DNA (ENSG00000147408). Quantitative SYBR green PCRs targeting 20 different loci from CSGALNACT1 intron 3 to intron 4, and normalized to ACTB as a control gene, were used to delineate the large intragenic deletion in P2 and to enable breakpoint sequencing. Primer sequences and PCR conditions are available from the authors upon request. Nucleotide numbering reflects complementary DNA numbering with +1 corresponding to the A of the ATG translation initiation codon in the reference sequence.

2.4 | In silico analysis of variants

The significance of SNVs resulting in missense changes was predicted using the following four web-based programs: Mutation Taster (<http://www.mutationtaster.org>), PolyPhen-2 (<http://genetics.bwh.harvard.edu/pph2/>), PROVEAN (<http://provean.jcvi.org/index.php/>), and CADD (complete annotation dependent depletion; <https://cadd.gs.washington.edu/>).

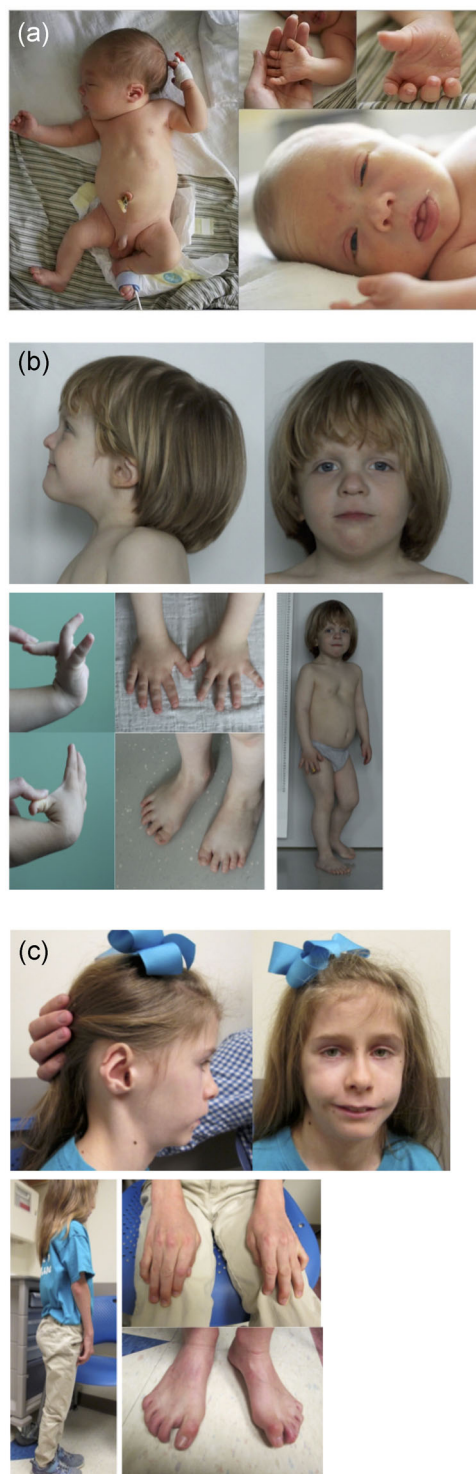


FIGURE 2 Clinical features in two unrelated patients with CSGALNACT1-CDG. (a) P2 at the age of 2 days presenting with relative macrocephaly with frontal bossing, midface hypoplasia, anteverted nares, downslanting palpebral fissures, ankyloglossia, dysplastic ears, rhizomelia, narrow chest, brachydactyly, and single palmar crease. (b) Aggravation of the phenotype with age. P2 at the age of 5 years showing marked disproportionate stature, macrocephaly, pectus excavatum, and skin laxity. (c) P3 at the age of 10 years with camptodactyly, mild skeletal anomalies and facial gestalt similar to P2 with short and downslanting palpebral fissures, midface hypoplasia, flat nasal bridge, prominent nasal tip, and dysplastic external ears

Variants were considered to be likely pathogenic if they had low allele frequencies (<0.005) in the normal population (ExAC database; <http://exac.broadinstitute.org/>), and were predicted to be damaging or disease-causing by at least three of four prediction programs, and segregated with the phenotype in the pedigree. Amino acid conservation was assessed by aligning a set of CSGALNACT1 orthologous protein reference sequences obtained from the NCBI database (<http://www.ncbi.nlm.nih.gov/gene/>) using ClustalOmega.

2.5 | Chromosomal microarray analysis

Chromosomal microarray analysis was performed in patients P2 and P3 using the genome-wide Human SNP Array 6.0, genotyping console 4.0, and ChAS 1.2.2 software (Affymetrix).

2.6 | Glycosyltransferase assay of recombinant, mutant, and wild-type CSGalNAcT-1

The human CSGalNAcT-1 (wild-type [WT]) expression vector, p3xFLAG-CMV8/hCSGALNACT1 was used to generate p.Asp432Tyr and p.Asn264Ser variants in CSGALNACT1 as described previously for patient P1 with the pPro384Arg CSGALNACT1 variant (Vodopituz et al., 2017). The variants were introduced by overlapping extension PCR (Zhao, Zhang, & Padmanabhan, 1993). The expression plasmid (6 µg) was transfected into HEK293T cells (~50% confluency) in a T-75 flask or 100-mm plate using FuGENE 6 HD (Promega) and GalNAc-transferase activity was determined as described (Uyama et al., 2002; Vodopituz et al., 2017). Briefly, the GalNAc-transferase assay mixture contained 10 µl of enzyme-bound anti-FLAG affinity resins, 50 mM 2-(N-morpholino)ethanesulfonic acid-NaOH (pH 6.5), 10 mM MnCl₂, 10 mM MgCl₂, 0.1 mM UDP-GalNAc (ultra-pure grade; Promega) as the sugar donor substrate, and 100 µg chondroitin (Seikagaku Corp., Tokyo, Japan) or 2 mM *p*-nitrophenyl-β-D-glucuronic acid (pNP-GlcUA; Sigma-Aldrich) as the sugar acceptor in a total volume of 50 µl. The reaction mixture was incubated at 37°C for 4 hr. The reaction product, the UDP moiety released from UDP-GalNAc, was mixed with UDP detection reagent, which contains an enzyme to convert UDP to adenosine triphosphate (ATP), in a UDP-Glo™ Glycosyltransferase Assay kit (Promega). The newly synthesized ATP was measured using a luciferase/luciferin reaction, and the luminescent signals were detected in a luminometer, Victor X4 or EnSpire (PerkinElmer).

2.7 | Primary fibroblast culture

Skin fibroblasts were available from patients P1 and P2. We cultured skin fibroblasts from patients and controls in Dulbecco's modified Eagle medium with 10% heat-inactivated fetal bovine serum, 100 U/ml penicillin, 100 U/ml streptomycin, and 2 mM L-glutamine (Invitrogen) in a humidified atmosphere containing 5% CO₂.

2.8 | Determination of the CS/DS chain number on core proteins by cell-based enzyme-linked immunosorbent assay (ELISA)

Cell-based ELISA was carried out as described (Job et al., 2016) to determine the relative number of CS/DS chains on core proteins. Briefly, fibroblasts from the patients and a control subject were cultured on 96-well plates (5,000 cells/well) for a day, washed with PBS, and treated with chondroitinase ABC at 37°C for 30 min. The chondroitinase-treated cells were fixed with 4% paraformaldehyde, incubated with the primary antibodies, a mixture of anti-CS-stub antibodies (1B5, 2B6, and 3B3, Cosmobio; Tokyo, Japan), and subsequently incubated with the secondary antibody, an alkaline phosphatase-conjugated anti-mouse immunoglobulin G. Then, the cells were incubated with the substrate, *p*-nitrophenyl phosphate, and analyzed by absorbance at 405 nm using an iMark microplate absorbance reader (Bio-Rad, Hercules, CA).

3 | RESULTS

3.1 | Genetic analysis

We generated sequencing reads for patients P2, P3, and parents of P3 yielding an average coverage of >120× with >95% of target sequenced at >20× coverage; sequencing reads for the parents of patient P2 yielded an average coverage of 40× with >82% of target sequenced at >20× coverage (low-coverage exomes). WES identified novel and biallelic *CSGALNACT1* variants in patients P2 and P3 with skeletal dysplasia with advanced bone age: P2 was compound-heterozygous for c.1294G>T (p.Asp432Tyr) and an intragenic deletion of 84,966 bp that removes exon 4 (NM_001130518.1:c.-297+17058_634+22070delinsT; Figures 3a,b and S1a). The *CSGALNACT1* expression level in fibroblasts from P2 was comparable to controls, with exon 4 missing in approximately half of the transcripts (Figure S1b,c and data not shown). Exon 4 contains the translation start codon as well as 211 out of 532 codons of *CSGALNACT1*. This deletion, therefore, precludes the synthesis of a functional *CSGALNACT1* protein and has not been reported in ClinVar and DECIPHER databases. Patient P3 was homozygous for c.791A>G (p.Asn264Ser), due to complete paternal isodisomy for chromosome 8, which harbors *CSGALNACT1*. The healthy father was heterozygous for this variant and the healthy mother was WT *CSGALNACT1* (Figure 3a,b and Table 1). The identified *CSGALNACT1* missense variants p.Asp432Tyr and p.Asn264Ser change evolutionary highly conserved amino acids (Figure 3c), are predicted to be damaging by multiple in silico algorithms, and all variants are very rare in the ExAC and gnomAD public databases (Table 1). WES did not reveal potentially pathogenic variants in any of the other known skeletal dysplasia genes in both patients, collectively indicating *CSGALNACT1* as the disease-causing gene. The *CSGALNACT1* variant information was submitted to the Leiden Open Variation Database. Chromosomal microarray analysis was normal in patient P2. Chromosomal microarray analysis of P3 revealed a region of homozygosity consistent with complete isodisomy of chromosome 8. WES data and clinical genetic testing of polymorphic DNA markers on chromosome

8 confirmed paternal isodisomy of chromosome 8 and interphase FISH (fluorescence in situ hybridization) revealed 3.5% mosaic trisomy 8 in leukocyte-derived DNA from P3 (Supplemental Fig. S2). P3 was also homozygous for a *VPS13B* variant NM_181661.2: c.1336_1351del, (p.Cys409Asnfs*5) due to paternal isodisomy 8. Recessive variants in *VPS13B* cause Cohen syndrome (MIM: 216550; Kolehmainen et al., 2003). However, we considered the *VPS13B* change as an unlikely cause of P3's phenotype; her clinical features do not overlap with Cohen syndrome and the variant only impacts a short alternate isoform.

3.2 | Patients' clinical characteristics

We performed detailed clinical assessment and analysis of skeletal radiographs for patients P2 and P3 (Figure 1) compared to the previously reported patients P1 (Vodopiutz et al., 2017) and P4 (Meyer et al., 2019; Table 1). The four patients with *CSGALNACT1* variants were all born at term and are now between 5 and 12-year old. Three patients displayed a fetal length below the fifth centile, and skeletal dysplasia was suggested prenatally in P1, P2, and P4 by short fetal femurs. An advanced bone age within the first year of life was observed in patients P1–3 (Figure 1a, b, m, o) and was reported at age 6 in P4. A mild spondyloepiphyseal dysplasia with short and plump long bones, flat acetabular roofs, and monkey wrench appearance of the proximal femur was documented in P1 and P2 (Figure 1a–l), for whom neonatal skeletal radiographs were available.

Relative macrocephaly, rhizomelia, hyperlordosis and joint laxity are present in P1, P2 and P4, whereas muscular hypotonia in infancy, mild neurodevelopmental delay, congenital heart defects, and dysplastic external ears are present in P2 and P3. Structural defects of the central nervous system, apnoes, and endocrine abnormalities are variable (Table 1).

3.3 | Case reports

The male patient P2 is the second child of healthy, nonconsanguineous northern European parents. P2 had cardiorespiratory monitoring at home in the first years of life due to the occurrence of apparent life-threatening events. At the age of 5 years 7 months, he has nonproportionate short stature, macrocephaly, brachydactyly, hyperlordosis, mild scoliosis, progressive pectus excavatum, pes planus, 2/3-toe syndactyly, and facial dysmorphism. Mild language delay and attention deficit hyperactivity disorder (ADHD) were noted. Cranial magnetic resonance imaging (MRI) showed mild ventriculomegaly, and reduced volumes of the hippocampi and cavum vergae. Electroencephalography, nerve conduction velocity studies, electromyography, metabolic and endocrine investigations were normal and family history is unremarkable (Figures 2a,b and 3a; and Table 1).

The female patient P3 is the second child of healthy, nonconsanguineous parents of Jewish and northern European descent (Figure 3a). At the age of 10 years, she presents with height at the third percentile, facial dysmorphism, scoliosis, overlapping fingers, 2/3-toe syndactyly, camptodactyly of the fifth distal interphalangeal joints, clinodactyly of second finger, and limited extension of elbows and

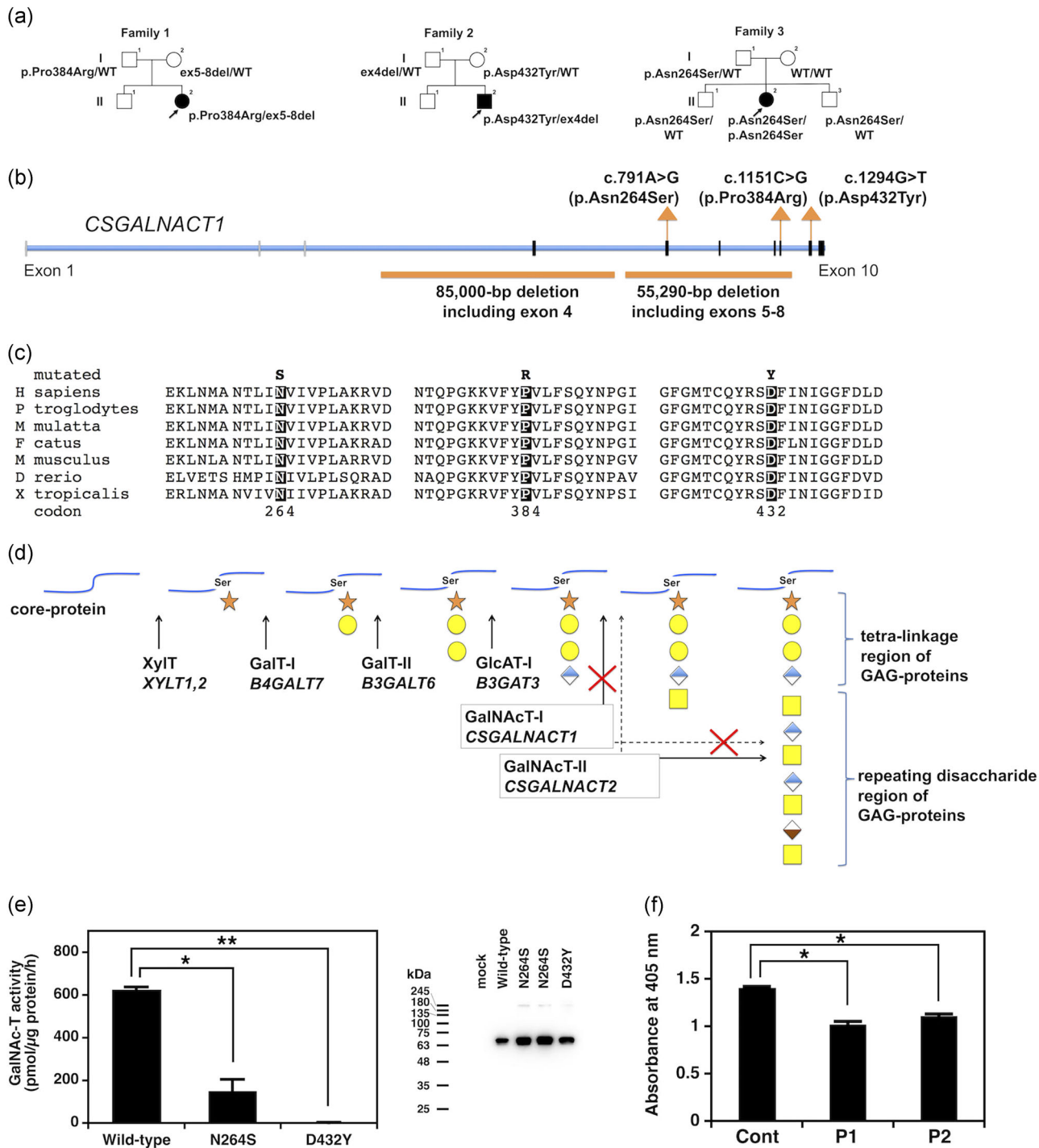


FIGURE 3 Identification and characterization of *CSGALNACT1* variants. (a) Simplified pedigrees showing segregation of identified *CSGALNACT1* variants. Individuals carrying biallelic *CSGALNACT1* variants are indicated by solid symbols, whereas unaffected individuals are indicated as open symbols. (b) Schematic of the human *CSGALNACT1* locus with exons displayed as gray (untranslated) and black (translated) boxes and the localization of reported and newly identified *CSGALNACT1* variants on complementary DNA and protein level indicated. (c) The two newly identified and one previously reported *CSGALNACT1* missense variants affect invariably conserved amino acids. (d) Schematic illustration of GAG synthesis with emphasis on *CSGALNACT1*. (e) In vitro GalNAc-transferase activities of p.Asp432Tyr-*CSGALNACT1* and of p.As264Ser-*CSGALNACT1* from cell lysates were significantly decreased towards chondroitin as the acceptor compared to that of wild-type (WT)-*CSGALNACT1*. Values are the means \pm standard error ($n = 3$). $*p < .0005$ and $**p < .0001$ versus WT were calculated by the analysis of variance (ANOVA) Dunnett test. Expression levels of the recombinant *CSGALNACT1* proteins were estimated by comparing the chemiluminescence intensity using the standard curve generated with concentration-defined 3 \times FLAG-bovine alkaline phosphatase. Two clones of variants p.As264Ser are shown. (f) CS/DS-stub antibodies showed a significantly reduced binding to patients' fibroblasts as compared to the control subject, indicating that the number of CS/DS chains were reduced in the fibroblast cells from P1 and P2. $*p < .0005$ versus control (Cont) were calculated by the ANOVA Dunnett test

TABLE 1 Clinical and genetic findings in four individuals with biallelic CSGALNACT1 variants

Patient (Reference)	P1 (Vodopitutz et al., 2017)	P2	P3	P4 (Meyer et al., 2019)
Sex	F	M	F	M
Ethnicity	Northern European	Northern European	Northern European/Jewish	Turkish
Parental consanguinity	-	-	-	+
Current age	5 years 7 months	5 years 10 months	10 years 5 months	12 years 3 months
Clinical characteristics				
Prenatal history	short femurs and midface hypoplasia	short femurs	Single umbilical artery, ventriculomegaly, high maternal serum AFP level	short femurs
Increased nuchal translucency	ND	+	-	-
Birth measures	HC 34.0 cm, P54, SD 0.1 W 2.826 g, P16, SD -0.97 H 46.5 cm, P8, SD -1.57 Apgar scores 9/10/10	HC 36.0 cm, P89, SD 1.2 W 3.610 g, P79, SD 0.76 H 48.0 cm, P15, SD -1.24 Apgar scores 9/10/10	HC 31.88 cm, P5, SD -1.69 W 2.056 g, P < 1, SD -2.6 H 43 cm, P < 3, SD -3.3 Apgar scores 7/8/ND	HC 35.5 cm, P75, SD 0.69 W 3.100 g, P46, SD -0.1 H 50.0 cm, P15, SD -1.24 Apgar scores not reported
Age and measurements at last follow-up	3 years 11 months HC 49.5 cm, P55, SD -0.14 H 95 cm, P13, SD -1.23 W 14.8 kg, P15, SD 0.79 SH ND SH/LL ND LL ND	5 years 7 months HC 56.7 cm, P > 97, SD 3.3 H 100.2 cm, P < 3, SD 3.03 W 19.0 kg, P40, SD -0.26 SH 59.3 cm, SD -1.69 SH/LL 1.45, SD 3.36 LL 40.9 cm, SD -3.62	10 years 5 months HC 51 cm, P10, SD -1.44 H 132.4 cm, P3, SD -1.77 W 23.8 kg, P < 3, SD -4.26 SH 77 cm, SD 0.59 SH/LL ND LL ND	12 years 3 months HC 54 cm, P34, SD -0.41 H 128 cm, P < 3, SD -3.14 W 32 kg, P6, SD -1.53 SH ND SH/LL ND LL ND
Neonatal respiratory distress	-	+	+	-
Apnoes/ALTE	-	+	-	-
Disproportionate stature	+	+	-	+
Short stature	-, 8-15, SD -1.23	+, 3P, SD -3.03	+, P3, SD -1.77	P < 3, SD -3.14
Brachydactyly	+	+	-	-
Macrocephaly	-	+, +3.3, SD	-	-
Single palmar crease	-	+	+	-
Facial dysmorphism		Midface hypoplasia, frontal bossing, flat nasal bridge, antverted nares at birth, beaked nose, prominent nasal	Downslanting and short palpebral fissures,	-

(Continues)

TABLE 1 (Continued)

Patient (Reference)	P1 (Vodopituz et al., 2017)	P2	P3	P4 (Meyer et al., 2019)
Joint laxity	+	+	-	+
Joint dislocations	-	-	+	-
Pectus excavatum	-	+	-	-
Scoliosis	-	+	+	-
Hyperlordosis	+	+	-	+
Other skeletal features	pes planus	2/3 toe syndactyly, clinodactyly, and pes planus	2/3 toe syndactyly, camptodactyly of fifth DIP joint, clinodactyly of second finger, limited extension at elbows and knees, and history of overlapping fingers	Pes planus and genua valga
Muscular hypotonia in early infancy	+	+	+	-
Mild motor delay	+	+	+	-
Language delay	-	+	+	-
Mild attention deficit hyperactivity disorder	ND	+	+	-
Eye	-	Hyperopia	Hyperopia, mild optic nerve anomaly, strabismus, and retinal pigment mottling	-
Miscellaneous	-	Ankyloglossia and nevus flammeus over both eyes	Clinical features of mosaic trisomy 8 Tethered cord, chilblain lesions, deafness conductive left side, Nevus flammeus over both eyes, deep plantar creases, bilateral deeply set eyes, feeding difficulties, widely spaced nipples, panhypopituitarism, and velopharyngeal insufficiency	-
Radiological characteristics				
Advanced carpotarsal bone age in infancy	+	+	+	+
	Vanished at age 4.5 years	Vanished at age 9 years	vanished at age 9 years	

(Continues)

TABLE 1 (Continued)

Patient (Reference)	P1 (Vodopituz et al., 2017)	P2	P3	P4 (Meyer et al., 2019)
Neonatal monkey wrench appearance femoral neck	+ Vanished at age 5 years	+ Vanished at age 4.5 years	ND	ND
Flat acetabular roofs	+	+	ND	+
Short long bones	+	+	-	-
Epiphyseal dysplasia	+	+	ND	-
Vertebral abnormalities	Coronal and sagittal clefting of vertebrae	Coronal clefting of vertebrae	Oar shaped ribs	-
Desbuquois dysplasia type 1; characteristic hand anomalies	-	-	-	-
Miscellaneous	-	Narrow chest	Radial head luxation and dysplasia	-
Bone densitometry	ND	Normal at 4.5 years	ND	ND
Brain MRI	Normal	Mild ventriculomegaly, cavum vergae, and mild bilateral volume loss in hippocampal region	Mild ventriculomegaly, agenesis of corpus callosum, periventricular gray matter heterotopia, absent septum pellucidum, and hypoplastic of inferior cerebellar vermis	ND
EEG	ND	Normal	Normal	ND
NCV	ND	Normal at age 2 months	ND	ND
Echocardiography	ND	ASD	VSD, history of patent ductus arteriosus, patent foramen ovale, abnormality of the tricuspid valve, tricuspid valve regurgitation	ND
CDG screening	Normal	Normal	Normal	ND
Genetics				
CSGALNACT1 variants (ACMG classification)	Compound-heterozygous c.1151C>G p.Pro384Arg (PS3, PS4, PM2, PM3: pathogenic) NC_000008.10:g.19269401_19324691del 55-kbp deletion, exons 5-8 (PV51, PS3, PM2, PM3: Pathogenic)	Compound-heterozygous c.1294G>T p.Asp432Tyr (PS3, PS4, PM2, PM3: pathogenic) NC_000008.10:g.19340642_19425619delinsA 85-kbp deletion, exon 4 (PV51, PS3, PS4, PM2, PM3, PM4: Pathogenic)	Homozygous c.791A>G p.Asu264Ser (PS3, PS4, PM2, PM3: Pathogenic)	Homozygous c.372del p.(His125Thrfs*9) (PV51, PM2, PM3: Pathogenic)
In silico algorithms ^a for PolyPhen-2 PROVEAN Mutation Taster	p.Pro384Arg Probably damaging (1.0) Deleterious (-8.298) Disease-causing	p.Asp432Tyr Probably damaging (1.0) Deleterious (-7.798) Disease-causing	p.Asu264Ser Probably damaging (1.0) Deleterious (-3.600) Disease-causing	p.(His125Thrfs*9) NA NA Disease-causing

(Continues)

TABLE 1 (Continued)

Patient (Reference)	P1 (Vodopitutz et al., 2017)	P2	P3	P4 (Meyer et al., 2019)
CADD PHRED	Deleterious (24.6) 3/121,819; 0	Deleterious (24.4) 0/121,108; 0	Deleterious (26.1) 14/121,412; 0	Deleterious 0/120,614; 0
Allele frequencies in ExAC (het.; hom.)	7/282,742; 0	0/251,406; 0	38/282,980; 0	0/250,398; 0
gnomAD (het.; hom.)				
Miscellaneous			Paternal isodisomy of chromosome 8; 3.5% mosaic trisomy 8 (46,XX/47,XX,+8)	

Abbreviations: ACMG, American College of Medical Genetics and Genomics; ALTE, apparent life-threatening events; CADD, complete annotation dependent depletion; CDG, congenital disorder of glycosylation; EEG, electroencephalogram; ExAC, Exome Aggregation Consortium; g.a., gestational age; gnomAD, genome aggregation database; H, height; HC, head circumference; LL, leg length; MRI, magnetic resonance imaging; NA, not applicable; NCV, nerve conduction velocity; ND, not determined; P, percentile; SD, standard deviation; SH, seat height; VSD, ventricular septal defect; W, weight. aDefault parameters were used; CADD scores were obtained from SeattleSeq (<http://snpgs.washington.edu/SeattleSeqAnnotation/>).

knees (Figure 2c). Mild language delay, specifically in expressive language, and ADHD were noted. MRI of the brain and spine at 2 days of life showed mild ventriculomegaly, agenesis of corpus callosum, periventricular gray matter heterotopia, absent septum pellucidum, hypoplastic inferior cerebellar vermis, and tethered cord. Electroencephalography and metabolic testing were normal. She has been treated with growth hormone for panhypopituitarism since age 7 years. She has tricuspid valve regurgitation and a small ventricular septal defect. Notably, she appears to have blended phenotypes of two different disorders as strabismus, camptodactyly, limited joint mobility, contractures, deep plantar and palmar creases, and corpus callosum aplasia are typical findings in mosaic trisomy 8 (for a review see <https://rarediseases.info.nih.gov/diseases/5359/mosaic-trisomy-8>; Figures 1m–o and 2c and Table 1).

3.4 | Identified CSGalNAct-1 missense variants confer loss-of-function in vitro

The function of CSGalNAct-1 in GAG synthesis is depicted in Figure 3d. We expressed p.Asp432Tyr, p.Asn264Ser, and WT encoding CSGalNAct-1 in HEK293T cells in soluble form by replacing the first 36 amino acids of CSGalNAct-1 with a cleavable preprotrypsin signal sequence as well as a 3×FLAG epitope to facilitate enzyme purification and elimination of endogenous CSGalNAct-1. The presence of the WT CSGalNAct-1, but not the mutant enzymes, was detected in the conditioned medium by immunoblotting (Figure S3). In contrast, the protein expression levels in the cell fraction were comparable between the WT and the mutant enzymes (Figures 3e and S3).

GalNac-transferase activities of p.Asp432Tyr-CSGalNAct-1 and of p.Asn264Ser-CSGalNAct-1 from the cell lysates toward chondroitin (Figure 3e) and toward pNP-GlcUA (Figure S3) were significantly decreased compared to WT-CSGalNAct-1 ($p < .0001$ and $p < .0005$, respectively). These data indicate that both CSGALNACT1 variants lead to a loss of enzyme function.

3.5 | GAG chain quantity and composition analyses in patients' fibroblasts

To examine how the reduced activity of CSGalNAct-1 affects the biosynthesis of CS/DS side chains of PGs, we determined the relative numbers of CS/DS chains in fibroblast cells from patients P1, P2, and the control. No fibroblasts were available from P3. CS/DS-stub antibodies showed a significantly reduced binding to the patients' cells compared to the control subject ($p < .0005$; Figure 3f).

To examine the level of GAGs in patients' cells, we carried out quantification of disaccharides from CS/DS chains by a combination of enzymatic digestion with an anion-exchange HPLC (Figures S4–6 and Tables S1–3). We observed increased levels of the CS moiety in the GAG fractions prepared from the conditioned media from both patients P1 and P2 compared to that of a healthy control (Figure S3). The amount of CS in the cell preparations increased in patient P2, whereas it decreased in patient P1 (Figure S4). In addition, we

observed a marked increase in the amounts of DS for the GAG fractions prepared from both conditioned media and cell preparations of both of the patients' cell cultures compared to the control fibroblasts (Figure S5 and Table S2).

These observations suggest an increase in the amounts of CS/DS synthesized by the patients' fibroblasts, consistent with previous results (Vodopiutz et al., 2017), although the numbers of CS/DS chains from the fibroblast cultures of the patients were reduced compared to control.

The amount of HS from the cell preparations of patients P1 and P2 increased compared to that from the control (Figure S6) and the amount of HS in conditioned medium of cells from patient 2 increased, whereas it decreased in patient P1, compared to that from the control fibroblasts (Figure S6 and Table S3).

4 | DISCUSSION

Aggregate data from our previous work (Vodopiutz et al., 2017), a current case report (Meyer et al., 2019), and this study show biallelic *CSGALNACT1* variants in four unrelated individuals who present with a mild skeletal dysplasia with an advanced bone age. Three of four patients (P1, P2, and P4) display nonproportionate short stature, hyperlordosis, pes planus, and mild joint laxity. Such a phenotype appears confounded by mosaic trisomy 8 in patient P3 who displays short stature. Language delay and ADHD, as well as variable facial dysmorphism, were seen in patients P2 and P3; whether any of these symptoms are also due to the biallelic *CSGALNACT1* variants is currently unclear. *CSGALNACT1* encodes CSGalNAcT-1 which regulates the initiation of CS/DS chain formation by enzymatically catalyzing the transfer of a GalNAc residue from UDP-GalNAc onto the linker region in the O-Xyl glycosylation pathway (Mizumoto, 2018; Mizumoto et al., 2015b; Uyama et al., 2002). In addition to detecting two large, inactivating *CSGALNACT1* deletions in patients, we showed that all three identified *CSGALNACT1* missense variants are loss-of-function variants by demonstrating significantly reduced CSGalNAcT-1 activities in vitro. A consequent decrease in CS/DS chain initiation activity was reflected in reduced numbers of CS/DS chains on core proteins in fibroblasts from patients P1 and P2, whereas the total amount of the CS/DS disaccharides was, unexpectedly, increased compared to control fibroblasts. The reduced CSGalNAcT-1 function thus leads to a reduced number of elongated CS/DS chains in fibroblasts, which might produce the connective tissue abnormalities in *CSGALNACT1*-CDG.

We were not able to study GAG alterations in cartilage, as no such patient material was available. However, we speculate that a decreased CSGalNAcT-1 activity would cause reduced numbers and/or decreased amounts of CS chains in cartilage, to produce the skeletal symptoms in patients. Our hypothesis is supported by studies of *Csgalnact1* knockout mice that exhibit reduced body length with significantly shortened long bones (humerus and tibia) when compared to WT mice, whereas the head circumference is of normal size. Additionally, *Csgalnact1*^{-/-} mice display mild neurocognitive

impairment (Yoshioka et al., 2017) and a reduction in CS content in cartilage and brain compared with WT mice, but have normal fertility and lifespan (Iida-Yonemochi et al., 2018; Sato et al., 2011; Watanabe et al., 2010; Yamada, Nadanaka, Kitagawa, Takeuchi, & Jinno, 2018). These mouse studies suggest that CSGalNAcT-1 is necessary for normal levels of endochondral ossification, and the decrease in CS amount in the cartilage growth plate causes a rapid degradation of the prominent CS-PG, aggrecan. CS-PGs are known for their roles in cartilage, connective tissue, and brain development and function (Sato et al., 2011; Shimbo et al., 2017; Watanabe et al., 2010; Yamada et al., 2018).

The clinical features in *CSGALNACT1*-CDG patients are milder than those caused by enzyme deficiencies, which are located upstream and downstream of CSGalNAcT-1 in GAG synthesis (Baasanjav et al., 2011; Bui et al., 2014; Dundar et al., 2009; Malfait et al., 2013; Nakajima et al., 2013; Unger et al., 2010). This might be explained by the fact that CSGalNAcT-1 deficiency can be widely compensated for by the functionally redundant enzyme CSGalNAcT-2. Our demonstration of a reduced total number but potentially elongated CS/DS chains in fibroblasts of *CSGALNACT1*-CDG patients is consistent with the original biochemical characterization of CSGalNAcT-1; CSGalNAcT-1 predominantly initiates CS chain synthesis by transfer of the first GalNAc residue, whereas CSGalNAcT-2 is supposed to elongate CS chains by transferring the second and subsequent GalNAc residues (Sato et al., 2003; Uyama et al., 2002, 2003). Recent experiments in a mouse model suggested that even additional CS synthases other than *Csgalnact1* and *Csgalnact2* might exist to initiate CS chain synthesis (Shimbo et al., 2017). The observed increase in HS levels in patients' fibroblasts (P1 and P2) is consistent with findings in *Csgalnact1* knockout mice where upregulation of HS chain synthesis has been demonstrated as well (Takeuchi et al., 2013), caused by accumulation of the tetrasaccharide linker, which functions as an acceptor substrate for the HS glycosyltransferases. It remains unclear whether an imbalance of CS/DS and HS chains contributes to the pathogenesis in *CSGALNACT1*-CDG.

Advanced bone age and monkey wrench appearance of the femur are radiographic features which are rare in other skeletal dysplasias but common in GAG-biosynthesis disorders due to *ACAN*, *XYLT1*, *CANT1*, and *IMPAD1* variants. *ACAN* encodes the CS-PG aggrecan, which is an important component of the cartilage matrix (Gkourgianni et al., 2017; Nilsson et al., 2014; Stattin et al., 2010; Tompson et al., 2009). *XYLT1* encodes for enzyme directly involved in synthesis and modification of PGs, similar to *CSGALNACT1* (Bui et al., 2014; Schreml et al., 2014), whereas *CANT1* and *IMPAD1* dysfunctions are supposed to negatively affect overall GAG synthesis by causing feedback inhibitions of several glycosyltransferases and sulfotransferases through increased UDP and adenosine-3',5'-bisphosphate levels in the Golgi apparatus, respectively (Huber et al., 2009; Vissers et al., 2011). Advanced bone age in *CSGALNACT1*-CDG might result from defective glycosylation of aggrecan and other CS-PGs in the cartilage matrix. Testing for PG biosynthesis defects is recommended in patients with skeletal dysplasia and advanced bone age or monkey

wrench appearance of the femur, especially if further symptoms of PG biosynthesis defects are present such as joint laxity, or neurodevelopmental delay. Vanishing of advanced bone age and monkey wrench appearance with age in CSGALNACT1-CDG highlights the importance of a complete neonatal radiographic work up in patients with unknown skeletal dysplasia.

Joint laxity is a common symptom in GAG biosynthesis disorders, and was noted in P1, P2, and P4 but was not present in P3 with an additional trisomy 8 mosaicism. Limited joint mobility is a characteristic feature of mosaic trisomy 8 and might counteract joint hypermobility in P3. A dislocated and dysplastic radial head was diagnosed in P3, but it is unclear if this is due to her GAG synthesis disorder, as this symptom has been reported in mosaic trisomy 8 (<https://rarediseases.info.nih.gov/diseases/5359/mosaic-trisomy-8>) as well as in the EXTL3-associated GAG synthesis disorder (Oud et al., 2017). Of note, none of the three patients presented with multiple congenital dislocations, which are typically seen in GAG biosynthesis defects located upstream and downstream of CSGALNACT1 (Dundar et al., 2009; Janecke et al., 2016; Nakajima et al., 2013; Unger et al., 2010).

In summary, the three unrelated individuals reported by us and an independent recent case indicate that biallelic CSGALNACT1 variants result in a mild skeletal dysplasia with advanced bone age. Our findings also expand the clinical spectrum of O-Xyl glycosylation pathway defects.

ACKNOWLEDGMENTS

We are grateful to the families who participated in this study for their enthusiasm and interest in our work. We thank Dr. Stephen P. Robertson (University of Otago) for experimental advice and Ms. Erica Phillips (Duke University Cytogenetics Laboratory) for help with clinical genetic testing. The study was supported by a grant from Jubiläumsfond Oesterreichische Nationalbank Nr17627 (to J. V.); in part by a Grant-in-Aid for Scientific Research (C) 16K08251 (to S. M.), 19K07054 (to S. M.) from the Japan Society for the Promotion of Science, Japan; by the Takeda Science Foundation (to S.M.); and U.S. National Institutes of Health grant DK096415 (to N. K.) and by a Grant-in Aid for Research Center for Pathogenesis of Intractable Diseases from the Research Institute of Meijo University (to S.M. and S.Y.) MH106826 (to E. E. D.)

CONFLICT OF INTERESTS

N. K. is a distinguished Jean and George Brumley Professor and a paid consultant for and holds significant stock of Rescindo Therapeutics, Inc. Remaining authors declare that there are no conflict of interests.

ORCID

Andreas R. Janecke  <http://orcid.org/0000-0001-7155-0315>

Nicholas Katsanis  <http://orcid.org/0000-0002-2480-0171>

Erica E. Davis  <http://orcid.org/0000-0002-2412-8397>

Julia Vodopituz  <http://orcid.org/0000-0002-8087-7026>

REFERENCES

- Baasanjav, S., Al-Gazali, L., Hashiguchi, T., Mizumoto, S., Fischer, B., Horn, D., & Hoffmann, K. (2011). Faulty initiation of proteoglycan synthesis causes cardiac and joint defects. *American Journal of Human Genetics*, *89*(1), 15–27.
- Bainbridge, M. N., Wang, M., Wu, Y., Newsham, I., Muzny, D. M., Jefferies, J. L., & Gibbs, R. A. (2011). Targeted enrichment beyond the consensus coding DNA sequence exome reveals exons with higher variant densities. *Genome Biology*, *12*(7), R68.
- Bishop, J. R., Schuksz, M., & Esko, J. D. (2007). Heparan sulphate proteoglycans fine-tune mammalian physiology. *Nature*, *446*(7139), 1030–1037.
- Bui, C., Huber, C., Tuysuz, B., Alanay, Y., Bole-Feysot, C., Leroy, J. G., & Cormier-Daire, V. (2014). XYLT1 mutations in Desbuquois dysplasia type 2. *American Journal of Human Genetics*, *94*(3), 405–414.
- Dundar, M., Muller, T., Zhang, Q., Pan, J., Steinmann, B., Vodopituz, J., & Janecke, A. R. (2009). Loss of dermatan-4-sulfotransferase 1 function results in adducted thumb-clubfoot syndrome. *American Journal of Human Genetics*, *85*(6), 873–882.
- Gkourogianni, A., Andrew, M., Tyzinski, L., Crocker, M., Douglas, J., Dunbar, N., & Dauber, A. (2017). Clinical characterization of patients with autosomal dominant short stature due to aggrecan mutations. *Journal of Clinical Endocrinology and Metabolism*, *102*(2), 460–469.
- Haltiwanger, R. S., & Lowe, J. B. (2004). Role of glycosylation in development. *Annual Review of Biochemistry*, *73*, 491–537.
- Huber, C., Oules, B., Bertoli, M., Chami, M., Fradin, M., Alanay, Y., & Cormier-Daire, V. (2009). Identification of CANT1 mutations in Desbuquois dysplasia. *American Journal of Human Genetics*, *85*(5), 706–710.
- Ida-Yonemochi, H., Morita, W., Sugiura, N., Kawakami, R., Morioka, Y., Takeuchi, Y., & Takeuchi, K. (2018). Craniofacial abnormality with skeletal dysplasia in mice lacking chondroitin sulfate N-acetylgalactosaminyltransferase-1. *Scientific Reports*, *8*(1), 17134.
- Izumikawa, T., Sato, B., Mikami, T., Tamura, J., Igarashi, M., & Kitagawa, H. (2015). GlcUA β 1-3Gal β 1-3Gal β 1-4Xyl(2-O-phosphate) is the preferred substrate for chondroitin N-acetylgalactosaminyltransferase-1. *Journal of Biological Chemistry*, *290*(9), 5438–5448.
- Janecke, A. R., Li, B., Boehm, M., Krabichler, B., Rohrbach, M., Muller, T., & Steinmann, B. (2016). The phenotype of the musculocontractural type of Ehlers-Danlos syndrome due to CHST14 mutations. *American Journal of Medical Genetics, Part A*, *170*(1), 103–115.
- Job, F., Mizumoto, S., Smith, L., Couser, N., Brazil, A., Saal, H., & Farrow, E. (2016). Functional validation of novel compound heterozygous variants in B3GAT3 resulting in severe osteopenia and fractures: Expanding the disease phenotype. *BMC Medical Genetics*, *17*(1), 86.
- Jordan, D. M., Frangakis, S. G., Golzio, C., Cassa, C. A., Kurtzberg, J., Task Force for Neonatal, G., & Katsanis, N. (2015). Identification of cis-suppression of human disease mutations by comparative genomics. *Nature*, *524*(7564), 225–229.
- Kolehmainen, J., Black, G. C., Saarinen, A., Chandler, K., Clayton-Smith, J., Traskelin, A. L., & Lehesjoki, A. E. (2003). Cohen syndrome is caused by mutations in a novel gene, COH1, encoding a transmembrane protein with a presumed role in vesicle-mediated sorting and intracellular protein transport. *American Journal of Human Genetics*, *72*(6), 1359–1369.
- Li, H., & Durbin, R. (2009). Fast and accurate short read alignment with Burrows-Wheeler transform. *Bioinformatics*, *25*(14), 1754–1760.
- Lindahl, U., & Rodén, L. (1965). The role of galactose and xylose in the linkage of heparin to protein. *Journal of Biological Chemistry*, *240*, 2821–2826.
- Malfait, F., Kariminejad, A., Van Damme, T., Gauche, C., Syx, D., Merhi-Soussi, F., & de Paepe, A. (2013). Defective initiation of glycosaminoglycan synthesis due to B3GALT6 mutations causes a pleiotropic Ehlers-Danlos-syndrome-like connective tissue disorder. *American Journal of Human Genetics*, *92*(6), 935–945.

- Meyer, R., Schacht, S., Buschmann, L., Begemann, M., Kraft, F., Haag, N., & Elbracht, M. (2019). Biallelic CSGALNACT1-mutations cause a mild skeletal dysplasia. *Bone*, 127, 446–451.
- Mizumoto, S. (2018). Defects in biosynthesis of glycosaminoglycans cause hereditary bone, skin, heart, immune, and neurological disorders. *Trend Glycosci Glycotechnol*, 30, E67–E89.
- Mizumoto, S., Yamada, S., & Sugahara, K. (2015a). Molecular interactions between chondroitin-dermatan sulfate and growth factors/receptors/matrix proteins. *Current Opinion in Structural Biology*, 34, 35–42.
- Mizumoto, S., Yamada, S., & Sugahara, K. (2015b). Mutations in biosynthetic enzymes for the protein linker region of chondroitin/dermatan/heparan sulfate cause skeletal and skin dysplasias. *BioMed Research International*, 2015, 861752.
- Nakajima, M., Mizumoto, S., Miyake, N., Kogawa, R., Iida, A., Ito, H., & Ikegawa, S. (2013). Mutations in B3GALT6, which encodes a glycosaminoglycan linker region enzyme, cause a spectrum of skeletal and connective tissue disorders. *American Journal of Human Genetics*, 92(6), 927–934.
- Ng, B. G., & Freeze, H. H. (2018). Perspectives on glycosylation and its congenital disorders. *Trends in Genetics*, 34(6), 466–476.
- Nilsson, O., Guo, M. H., Dunbar, N., Popovic, J., Flynn, D., Jacobsen, C., & Dauber, A. (2014). Short stature, accelerated bone maturation, and early growth cessation due to heterozygous aggrecan mutations. *Journal of Clinical Endocrinology and Metabolism*, 99(8), E1510–E1518.
- Oud, M. M., Tuijnburg, P., Hempel, M., van Vlies, N., Ren, Z., Ferdinandusse, S., & Kuijpers, T. W. (2017). Mutations in EXTL3 cause neuro-immuno-skeletal dysplasia syndrome. *American Journal of Human Genetics*, 100(2), 281–296.
- Povysil, G., Tzika, A., Vogt, J., Haunschmid, V., Messiaen, L., Zschocke, J., & Wimmer, K. (2017). panelcn.MOPS: Copy-number detection in targeted NGS panel data for clinical diagnostics. *Human Mutation*, 38(7), 889–897.
- Sato, T., Gotoh, M., Kiyohara, K., Akashima, T., Iwasaki, H., Kameyama, A., & Narimatsu, H. (2003). Differential roles of two N-acetylgalactosaminyltransferases, CSGalNACT-1, and a novel enzyme, CSGalNACT-2. Initiation and elongation in synthesis of chondroitin sulfate. *Journal of Biological Chemistry*, 278(5), 3063–3071.
- Sato, T., Kudo, T., Ikehara, Y., Ogawa, H., Hirano, T., Kiyohara, K., & Narimatsu, H. (2011). Chondroitin sulfate N-acetylgalactosaminyltransferase 1 is necessary for normal endochondral ossification and aggrecan metabolism. *Journal of Biological Chemistry*, 286(7), 5803–5812.
- Schremel, J., Durmaz, B., Cogulu, O., Keupp, K., Beleggia, F., Pohl, E., & Ozkinay, F. (2014). The missing “link”: An autosomal recessive short stature syndrome caused by a hypofunctional XYLT1 mutation. *Human Genetics*, 133(1), 29–39.
- Shen, Y., Wan, Z., Coarfa, C., Drabek, R., Chen, L., Ostrowski, E. A., & Yu, F. (2010). A SNP discovery method to assess variant allele probability from next-generation resequencing data. *Genome Research*, 20(2), 273–280.
- Shimbo, M., Suzuki, R., Fuseya, S., Sato, T., Kiyohara, K., Hagiwara, K., & Takahashi, S. (2017). Postnatal lethality and chondrodysplasia in mice lacking both chondroitin sulfate N-acetylgalactosaminyltransferase-1 and -2. *PLOS One*, 12(12), e0190333.
- Sobreira, N., Schiettecatte, F., Valle, D., & Hamosh, A. (2015). GeneMatcher: A matching tool for connecting investigators with an interest in the same gene. *Human Mutation*, 36(10), 928–930.
- Stattin, E. L., Wiklund, F., Lindblom, K., Onnerfjord, P., Jonsson, B. A., Tegner, Y., & Aspberg, A. (2010). A missense mutation in the aggrecan C-type lectin domain disrupts extracellular matrix interactions and causes dominant familial osteochondritis dissecans. *American Journal of Human Genetics*, 86(2), 126–137.
- Takeuchi, K., Yoshioka, N., Higa Onaga, S., Watanabe, Y., Miyata, S., Wada, Y., & Igarashi, M. (2013). Chondroitin sulphate N-acetylgalactosaminyl-transferase-1 inhibits recovery from neural injury. *Nature Communications*, 4, 2740.
- Tompson, S. W., Merriman, B., Funari, V. A., Fresquet, M., Lachman, R. S., Rimoin, D. L., & Krakow, D. (2009). A recessive skeletal dysplasia, SEMD aggrecan type, results from a missense mutation affecting the C-type lectin domain of aggrecan. *American Journal of Human Genetics*, 84(1), 72–79.
- Unger, S., Lausch, E., Rossi, A., Megarbane, A., Sillence, D., Alcausin, M., & Superti-Furga, A. (2010). Phenotypic features of carbohydrate sulfotransferase 3 (CHST3) deficiency in 24 patients: Congenital dislocations and vertebral changes as principal diagnostic features. *American Journal of Medical Genetics. Part A*, 152A(10), 2543–2549.
- Uyama, T., Kitagawa, H., Tamura Ji, J., & Sugahara, K. (2002). Molecular cloning and expression of human chondroitin N-acetylgalactosaminyl-transferase: The key enzyme for chain initiation and elongation of chondroitin/dermatan sulfate on the protein linkage region tetrasaccharide shared by heparin/heparan sulfate. *Journal of Biological Chemistry*, 277(11), 8841–8846.
- Uyama, T., Kitagawa, H., Tanaka, J., Tamura Ji, J., Ogawa, T., & Sugahara, K. (2003). Molecular cloning and expression of a second chondroitin N-acetylgalactosaminyltransferase involved in the initiation and elongation of chondroitin/dermatan sulfate. *Journal of Biological Chemistry*, 278(5), 3072–3078.
- Vissers, L. E., Lausch, E., Unger, S., Campos-Xavier, A. B., Gilissen, C., Rossi, A., & Superti-Furga, A. (2011). Chondrodysplasia and abnormal joint development associated with mutations in IMPAD1, encoding the Golgi-resident nucleotide phosphatase, gPAPP. *American Journal of Human Genetics*, 88(5), 608–615.
- Vodopiutz, J., Mizumoto, S., Lausch, E., Rossi, A., Unger, S., Janocha, N., & Janecke, A. R. (2017). Chondroitin sulfate N-acetylgalactosaminyl-transferase-1 (CSGalNACT-1) deficiency results in a mild skeletal dysplasia and joint laxity. *Human Mutation*, 38(1), 34–38.
- Watanabe, Y., Takeuchi, K., Higa Onaga, S., Sato, M., Tsujita, M., Abe, M., & Igarashi, M. (2010). Chondroitin sulfate N-acetylgalactosaminyltransferase-1 is required for normal cartilage development. *Biochemical Journal*, 432(1), 47–55.
- Yamada, J., Nadanaka, S., Kitagawa, H., Takeuchi, K., & Jinno, S. (2018). Increased synthesis of chondroitin sulfate proteoglycan promotes adult hippocampal neurogenesis in response to enriched environment. *Journal of Neuroscience*, 38(39), 8496–8513.
- Yoshioka, N., Miyata, S., Tamada, A., Watanabe, Y., Kawasaki, A., Kitagawa, H., & Igarashi, M. (2017). Abnormalities in perineuronal nets and behavior in mice lacking CSGalNACT1, a key enzyme in chondroitin sulfate synthesis. *Molecular Brain*, 10(1), 47.
- Zhao, L. J., Zhang, Q. X., & Padmanabhan, R. (1993). Polymerase chain reaction-based point mutagenesis protocol. *Methods in Enzymology*, 217, 218–227.

SUPPORTING INFORMATION

Additional supporting information may be found online in the Supporting Information section.

How to cite this article: Mizumoto S, Janecke AR, Sadeghpour A, et al. CSGALNACT1-congenital disorder of glycosylation: A mild skeletal dysplasia with advanced bone age. *Human Mutation*. 2020;41:655–667. <https://doi.org/10.1002/humu.23952>